CYCLIC VARIABILITY CORRELATIONS TO OPERATING CONDITIONS FOR SPARK-IGNITION ENGINES

Mohamed I. Amin[1,*], Ali Elmaihy[1], Moatasem Shahin[2]

[1]Mechanical Power Engineering Department, Military Technical College, Cairo, Egypt
[2]Mechanical Engineering Department, School of Engineering, Badr University of Cairo, Cairo, Egypt

*E-mail of corresponding author: mamin@mtc.edu.eg

Mohamed I. Amin 0000-0002-4348-6595, Ali Elmaihy 0000-0002-3917-9533,
Moatasem Shahin 0000-0003-3662-2453

Resume

Variations of successive combustion cycles are associated with power losses, vibration and fluctuations in the engine speed, torque and work done. Previous studies declared that the elimination of cycle-to-cycle variation (CCV) could improve the engine power by 10%. This work aims at correlating cyclic variability to engine operating conditions to determine the relevant operating conditions that affect the CCV and help designers to predict it. Experimental work was carried out on spark ignition, 4-stroke, 4-cylinder, 2.2 liters, with an 8.85:1 compression ratio and a maximum power of 85 kW at 5,000 rpm. The cyclic variability of many indicators is calculated from the measured in-cylinder pressure data. Results have been used to introduce new correlations considering the effect of normalized speed and load on cyclic variability with acceptable fit. These correlations could be a useful tool in early design calculations, CCV modeling and control.

Article info

Received 11 December 2022
Accepted 10 February 2023
Online 24 March 2023

Keywords:

spark ignition engines
cyclic variability
engine speed
engine load
compression ratio

Available online: https://doi.org/10.26552/com.C.2023.035

ISSN 1335-4205 (print version)
ISSN 2585-7878 (online version)

1 Introduction

Cyclic variability in spark-ignition engines causes a drop in overall engine performance and high emissions [1]. So, the control of Cycle-to-Cycle Variation (CCV) becomes a main target in the research field to improve engine efficiency and diminish their emissions.

Indicators have been developed to quantify the cyclic variability in internal combustion engines [2-5]. Based on these works, the CCV can be characterized by (i) the variation in pressure-related parameters; maximum pressure $(P_{\max})$, crank angle at maximum pressure $(\theta_{P_{\max}})$, maximum rate of pressure rise $\left[\frac{dP}{d\theta}\right]_{\max}$, the crank angle at the maximum rate of pressure rise $\left(\theta(\frac{dp}{d\theta})_{\max}\right)$, or coefficient of variance in indicated mean effective pressure (COV_{IMEP}), (ii) the concentration of exhaust gases components; (HC), (CO) or (NO_x), (iii) flame front-related parameters; flame front position (L), crank angle lapse between the flame front arrivals to two pre-specified different locations in the cylinder θ_{L1-2}, displacement of the flame kernel center from the spark gap at different crank angles $\left(\frac{dc}{d\theta}\right)$, or (iv) combustion related parameters; maximum rate of heat release $\left(\frac{dQ}{d\theta}\right)_{\max}$, maximum rate of mass burning $\left(\frac{dX_b}{d\theta}\right)_{\max}$, ignition delay $\Delta\theta_d$, combustion duration $\Delta\theta_b$, or time elapse from ignition to a moment, at which a certain mass fraction is burnt $\Delta\theta_{Xb}$.

Factors that influence the cyclic variability in the SI engines have been extensively studied during the last couple of decades. Authors have identified factors affecting the CCV to include mixture composition factors, cylinder charge factors, spark factors and in-cylinder mixture motion factors. Chemical (combustion-related factors) and physical (operating conditions and engine geometry) factors have also been ascribed to CCV. It is a common opinion [6-8], that the higher the laminar flame propagation velocity for a given type of fuel, the higher is the burning rate and the less is the CCV due to the combustion process. Examination of the overall equivalence ratio reveals [9-11] that minimum CCV occurs at a slightly rich mixture equivalence ratio (1-1.2) [12], which gives the shortest combustion duration and the highest peak pressure. Fraction of diluent studies, some of them incorporating skip firing to vary scavenging, confirm that the higher the diluent concentration the less is the burning rate and the greater the CCV [13-15]. This observation reveals the criteria for minimizing the NO_x emissions through the exhaust gas recirculation and the criteria for minimizing the CCV conflict. Mixture non-homogeneity as a result of imperfect fuel atomization and evaporation process, or as a result of poor mixing between the fresh charge and residual gases, repeatedly yields the conclusion that as mixture non-homogeneity increases, cyclic variability increases due to lower growth of pressure rate and predominant deceleration of flame propagation speed [16-18]. However, Ozdor [5] declares that the effect of inhomogeneity is still uncertain because its effect depends, to a large extent, on the turbulence intensity and scales.

The factors mentioned in the previous paragraph relate to mixture composition. Ignition-related factors follow. Examination of spark timing results [9, 19-21] yields a common conclusion that the minimum CCV can be achieved when ignition occurs at maximum break torque (MBT). Investigations of spark discharge characteristics, which means spark duration and energy, lead to two conflicting conclusions. First, the quicker the flame kernel reaches a critical size, as affected by the high spark energy, the lower is combustion-related cyclic variability [20, 22]. Second, spark discharge characteristics have been concluded not to affect the CCV, as long as the mixture can be ignited [5, 21, 23-24]. Spark plug design may influence the CCV through the shape and number of electrodes by affecting the flame/plug contact area fraction and thereby affecting flame kernel heat loss and through the spark gap by affecting the flame kernel development [24-26]. Some authors find no effect of electrode geometry on the standard deviations in burning times of the smallest flame kernel [27]; while others confirmed that fewer variations, especially in terms of the CCV_{IMEP} are experienced for cylinders equipped with four electrode plugs. Spark plug number and location have a strong influence on cyclic combustion variations [28]. Any change in these parameters decreases the maximum flame travel distance or increases the rate of mass burning and hence, decreases the flame travel times, resulting in lower cyclic variations [29].

The CCV factors related to in-cylinder mixture motion are described next. Due to the probabilistic nature of in-cylinder turbulence motion, investigators consider in-cylinder mixture motion as the major cause of the CCV that hampers engine performance. The mean flow velocity in the vicinity of the spark gap has a dominant effect on the very early stage of sparking and flame initiation; it affects the flame kernel growth rate through an alteration of spark characteristics and flame kernel convection [30-32]. Investigations of spark plug orientation, concerning the mean velocity vector, result in the observations that the cross-flow orientations produce the lowest levels of cyclic variability in indicated mean effective pressure (IMEP), while an upstream orientation produces the highest [33-34]. It is believed that turbulence intensity and scales affect combustion by wrinkling and corrugating the flame front, thus increasing flame surface area [35]. Nishiyama et al. [36] commented that the level of turbulence intensity near the spark gap should be increased up to a certain limit, depending on operating conditions and engine geometry. Above this limit, excessive flame stretching occurs causing the local flame quenching and increased CCV. Overall, in-cylinder flow pattern affects the CCV through early flame kernel convection and turbulence generation. Authors [37-39] provide different conclusions regarding swirl, tumble and squish motions, but the most common conclusion is that the swirl motion can provide a significant decrease in cyclic variability as measured by CCV in pressure, combustion development, burning rate and IMEP.

Sources of CCV have been hypothesized and discussed by different authors [5, 21, 40]. It is a common opinion that cyclic variability in turbulence intensity, cyclic variability of in-cylinder mixture homogeneity, cycle-to-cycle variation in velocity pattern inside the cylinder, cycle-to-cycle variation of mixture composition and cyclic variability in spark discharge characteristics are the main sources of CCV in combustion cycles.

Previous studies [41-42] show different approaches to model combustion and in-cylinder combustion process CCV. Some authors investigated the effect of displacement of the flame kernel on CCV in combustion. Others studied the turbulence variations, manifold pressure and residual gas effect on cycle-to-cycle variations in flame development using different approaches like the Auto-Regressive Moving Average (ARMA) technique.

It is a very complex and difficult task to quantify and control the cyclic variability phenomena given their dependence on such a large number of factors. To determine the lowest number of relevant independent factors, needed to be controlled to control CCV, it is mandatory to investigate them individually and in a factorial manner. Although most of these factors depend, more or less, on operating parameters, there is no explicit relation that quantifies cyclic variability in terms of operating parameters. This work aims to study the effect of operating parameters (speed, load), rather than one design parameter (compression ratio) on CCV experimentally. Moreover, empirical relations that predict the cyclic variability in terms of operating parameters are introduced. Such investigation could be an important step for engine assessment and cyclic variability phenomena prediction, modelling and control.

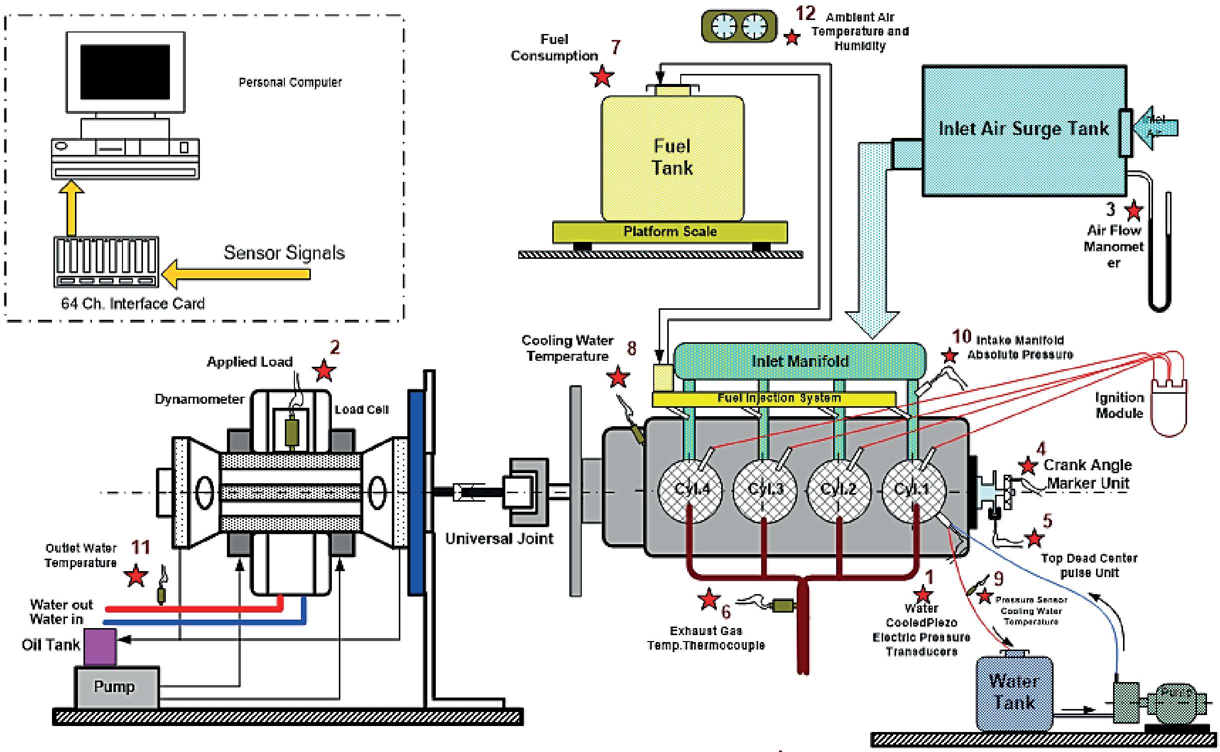

***Figure 1** Schematics of the test rig*

2 Experimental setup and program

The first stage of this research work was to erect a modern test rig for the study of the characteristics of spark-ignition engines. The test rig included an engine and the instrumentation that was necessary for measuring and recording the parameters important to engine performance and combustion. The experimental investigations were conducted on a General Motors four-stroke, four-cylinder water-cooled spark-ignition engine. The engine capacity was 2.2 litres, with an 8.85:1 compression ratio, 115 horsepower maximum power at 5,000 rpm and 183 Nm maximum torque at 3,600 rpm. The engine external load was applied by a Go-Power Systems hydraulic dynamometer; model D-356, with water as the working fluid. The maximum braking torque could reach 690 Nm at 3,000 rpm. Figure (1) gives a general schematic of the complete test rig with the locations of the used sensors and transducers. The positions of measuring transducers and pickups (relevant to Figure 1) with their main specifications are listed in Table 1.

The data acquisition system, which was used in this work, is a 64-input channel online system for recording the slowly and quickly varying parameters. The system operates in a sequence of input channel multiplexing, signal sampling and holding, analogue to digital conversion and finally, storing the digital result. This sequence is controlled, step by step, by a computer, which at the end of each measuring procedure stores the test data. The used card is an NI input-output data acquisition one type PCI-6071E with 64 analogue inputs A/D channels and two outputs D/A channels. The resolution of this card is 12 bits. The sampling rate of the A/D channels is software adjustable with a maximum 1.25 MHz rate. The Lab-View software was used in acquiring and saving the data. The acquisition rate, start and duration of acquisition, number of channels and data storage processes, were controlled through the program. To keep the acquisition process as fast as possible, this program was used for acquiring and saving only; another MATLAB program was written for later data analysis.

At the beginning of this work, 600 to 1,000 successive data cycles were acquired in each test. The resulting data was then divided into batches, each containing the pressure data for 25 successive cycles. The standard deviations and the coefficient of variance of the IMEP were then repeatedly evaluated for the first group of cycles, which contained an increasing multiple of 25 cycles. It is evident that both the coefficient of variance and the standard deviation become almost constant after 300 cycles, as shown in Figure (2). Therefore, it was concluded that it is necessary to investigate the data of at least 300 successive cycles to study the cyclic variability problem.

Steady-state tests were carried out under different operating conditions: namely engine speed and brake load. At each engine speed of 1,000, 1,500, 2,000, 2,500 and 3,000 rpm, data acquisition was performed at specific brake loads, namely 00, 27.1, 54.2, 81.35, 108.35, 135.58 and 162.7 N.m. These values of speed

Table 1 *The measured parameters with their corresponding measuring instruments, accuracies and uncertainties (Measured Point no. is pertinent to Figure 1).*

Meas. Point No	Measured Parameter	Instrument	Range	Accuracy	Uncertainty (%)
1	Cylinder Pressure	6041A Kistler Water-Cooled Pressure Transducer	0 - 250 bar	Th. Sens. < ± 0.5%. Linearity 0.5% OFS. Hysteresis 0.5% OFS	± 0.2%
10	Intake manifold absolute pressure	PX-203 OMEGA Absolute Pressure Transducer	0-206.8 kpa	0.25% FS. Th. effect 0.009% FS/1F	NA
4	Crank Angle and Engine Speed	Encoder (WD GI 58B)	1 pulse/ 0.25 ° CA to 1 pulse/ 1 ° CA.)	Phase Shift 90° ± max. 7. 5% of the period duration. pulse-/pause-ratio ≤ 5000 ppr: 50% ± max. 7%	± 0.6%
2	Load cell reading	Load Cell Central CTD2-300	1334.5 N	< 0.05% OFS. Th. shift < 0.09% FS/C	± 0.1%

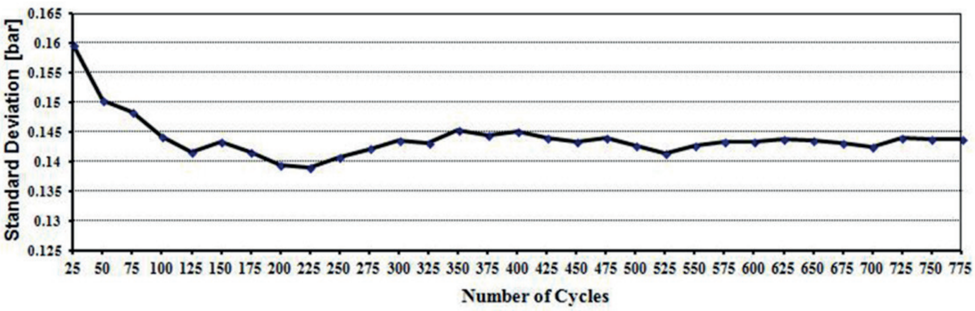

(A) Applied Load = 54.2 Nm, Engine Speed = 1,000 rpm

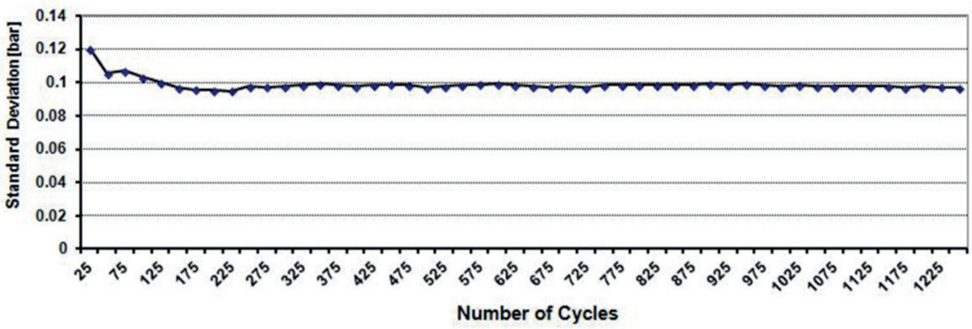

(B) Applied Load = 27.1 Nm, Engine Speed = 1,500 rpm

Figure 2 *Sample of the IMEP standard deviation in terms of number of successive cycles at different operating conditions*

and load were chosen to cover the widest range of engine operation (35 combinations) and thus increase, as much as possible, the range of the cyclic variability investigation. In each test, the in-cylinder pressure, crank angle and TDC marker data were acquired and retained for 300 successive cycles. Engine speed and load, in addition to fuel and air consumption, exhaust temperature and intake manifold absolute pressure, were monitored and recorded, as well.

3 Results and discussion

3.1 Effect of external applied load and engine speed on cyclic variation

Heywood [4] defined the coefficient of variance of indicated mean effective pressure (COV_{IMEP}) as an important indicator of the cyclic variability. This variable is defined as the ratio of the standard deviation

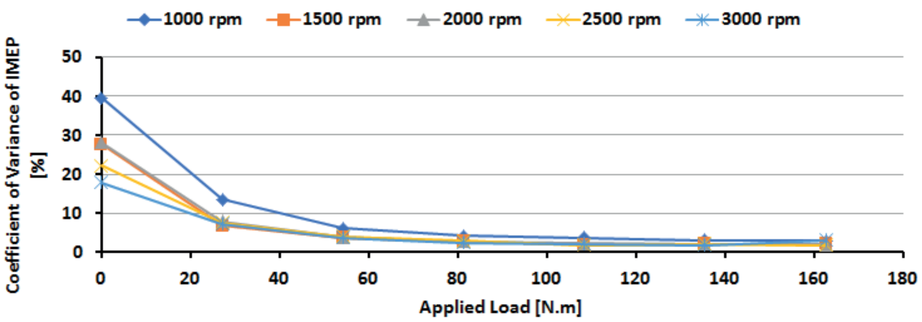

Figure 3 *Dependence of the* COV_{IMEP} *on applied load at different engine speeds*

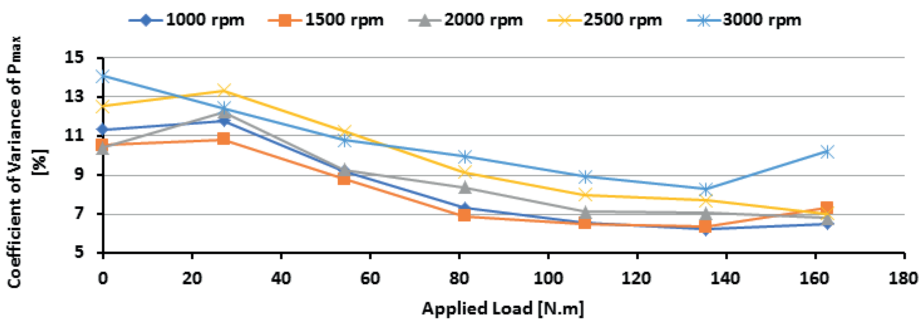

Figure 4 *Dependence of the COV of maximum pressure on applied load at different engine speeds*

in the indicated mean effective pressure (σ_{IMEP}) over many successive cycles divided by its mean value and is usually expressed as a percentage as follows:

$$COV_{IMEP} = \frac{\sigma_{IMEP}}{IMEP} * 100\%, \quad IMEP = \frac{\oint PdV}{Swept\, Volume}. \tag{1}$$

Figure 3 indicates the dependence of the COV of the IMEP on the externally applied loads [Nm] at constant speeds. The values of the COV are almost constant at loads higher than 30 Nm, irrespective of engine speed. However, at lower loads, the COV progressively increases, especially at engine speeds below 1500 rpm. The negative effect at low loads can be attributed to the increased amount of residual gases remaining in the combustion chamber at the end of the scavenging period, which leads to lower combustion flame speed. Besides this negative effect, there is the negative effect of the valve overlap at low engine speeds accounts for the increased COV at 1000 rpm. In addition, at near idle conditions (low engine speeds and low loads), the low level of turbulence results in a poor premixing of the fresh charge and higher cyclic variations.

The effect of the engine load on the COV of the maximum value of the cylinder pressure at constant speeds is depicted in Figure 4. It is evident that the COV increases slightly as the loads decrease to lower than 30 Nm, the same trend as the COV_{IMEP}.

Figures 5 to 7 summarize the effects of load on the cylinder pressure history at constant speeds and show that the combustion process is greatly disturbed at low loads. This is manifested in the large relative changes in the timing ($\theta_{P\max}$) of the maximum cylinder pressure, as shown in Figure 5. Consequently, the expansion process, represented by expansion polytropic exponent n_2, is affected, especially at low loads, Figure 7. On the other hand, Figure 6 proves that the compression curve, represented by compression polytropic exponent n_1, is only slightly affected at low loads. It is believed that this is a result of the ignition point changing and the beginning of the combustion process.

The effects of the engine speed on the COV of the various parameters seem to be relatively small at all the loads except close to idle conditions (low speed and low load). This supports the previous analysis and confirms that cyclic variability is practically experienced at speeds below 1,500 rpm and external braking loads less than 30 N.m. This is seen in Figures 5 to 7, where there are no significant changes at different speeds except at low loads.

3.2 Correlating cyclic variations to engine speed and external load

Previous results and discussion show that the cyclic variations are dependent on engine speed and external load. Other design characteristics, such as the compression ratio, valve timing and ignition and fuel system parameters, are expected to contribute to the cyclic variations. Further investigations of these parameters need to be conducted in a factorial manner to provide a complete map of the CCVs.

The IMEP value is affected mainly by the pressure-

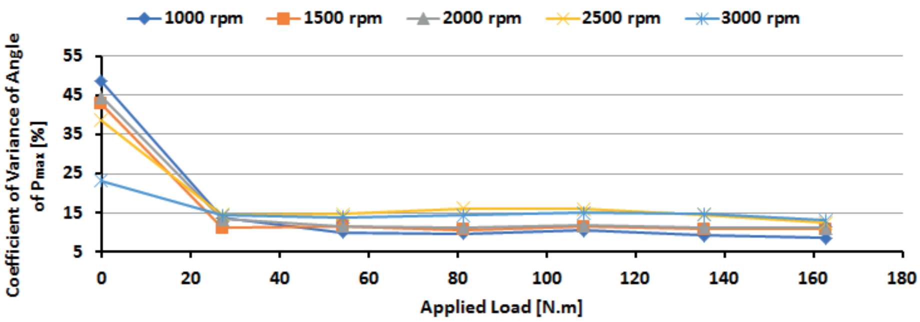

Figure 5 *Dependence of the COV of $\theta_{P\max}$ on applied load at different engine speeds*

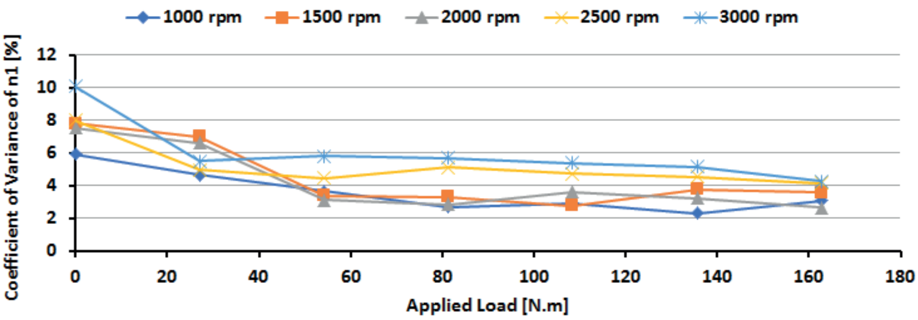

Figure 6 *Dependence of the COV of compression polytropic exponent (n_1) on applied load at different engine speeds*

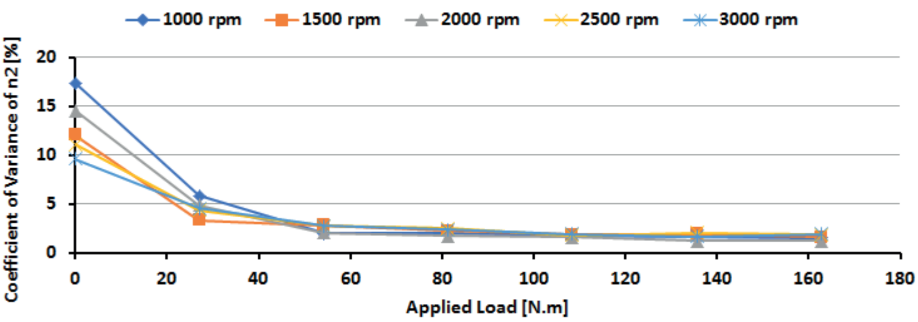

Figure 7 *Dependence of the COV of expansion polytropic exponent (n_2) on applied load at different engine speeds*

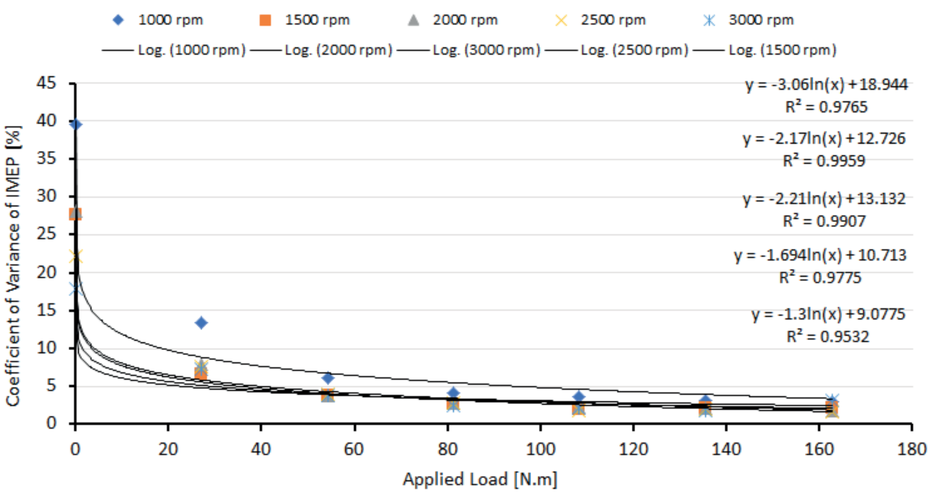

Figure 8 *Trend lines of the COV_{IMEP} dependence on applied load at constant speeds*

Table 2 *Correlation formulae of the COV of characterizing parameters*

Correlation Formulae	R^2	Standard Error	Significance F
$COV_{IMEP} = -0.678\frac{\ln(v)}{v} + 7.1436\frac{e^{-9.73\mu}}{v} - 9.311\left(\frac{\mu}{v}\right)^{0.18} + 10.993$	0.987813	1.046008	9.7E-30
$COV_{P_{max}} = -102.33(\nu) - 81.651(\mu) + 103.287(\nu)^{1.1} - 7.0551(e^{-12\mu}) + 71.0315(\mu)^{1.25} + 21.191$	0.942634	0.584337	4.33E-17
$COV_{\theta P_{max}} = 256.629(\nu) + 25.3746(\mu) - 128.94(\nu)^2 - 55.889\ln(\nu) + 8.76612\left(\frac{e^{-12\mu}}{\nu}\right) - 19.025(\mu)^2 - 16.599\left(\frac{\mu}{\nu}\right)^{0.12} - 113.28$	0.953413	2.516873	2.56E-16
$COV_{n1} = -31.412(\nu) - 29.104(\mu) + 24.0818(\nu)^2 + 52.0949(\mu)^2 - 29.125\mu^3 + 0.99789\left(\frac{Ln(\nu)}{\nu}\right) - 0.3357\left(\frac{\mu}{\nu}\right) - 0.6793\left(\frac{e^{-14\mu}}{\nu}\right) + 20.0566$	0.870005	0.748355	1.15E-09
$COV_{n2} = -0.1108\frac{Ln(v)}{v} + 2.62169\left(\frac{e^{-9\mu}}{v}\right) - 5.5041\left(\frac{\mu}{v}\right)^{0.16} + 7.26$	0.973009	0.694006	2.17E-24

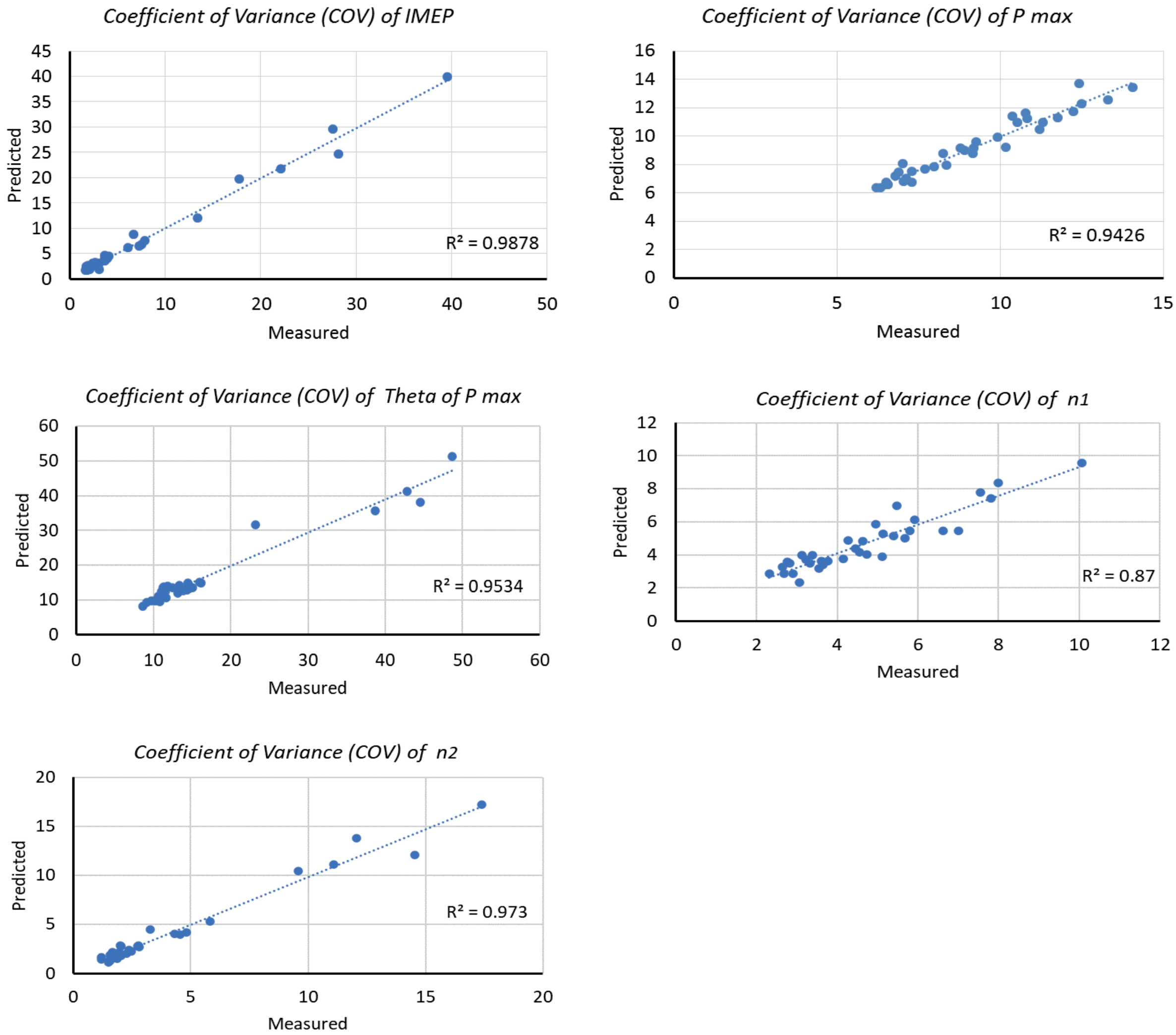

Figure 9 *Measured VS predicted COV of different characterizing parameters*

volume diagram characterizing parameters, such as the maximum pressure P_{max}, the crank angle at which maximum pressure occurs $\theta_{P_{max}}$, compression polytropic exponent n_1 and expansion polytropic exponent n_2. So, it is convenient to investigate the effect of operating conditions (speed and load) on these characterizing parameters variation.

Figure 8 displays the dependence of the COV of the IMEP on the externally applied load with the trend lines drawn at constant engine speeds. Several attempts are made to obtain a sound mathematical dependence of the COV on the engine load, with different degrees of success. The best results are obtained when the dependence is assumed to take a logarithmic form as suggested by the shapes of the trend lines. The least-square curve fitting techniques are used to evaluate the coefficients of the assumed equation, which gives the minimum residuals ($R^2 > 0.95$).

The procedure that was previously followed is repeated to correlate the characterizing parameters variations and operating conditions of the engine. These steps provide guidelines about the nature of relations. Regression techniques are then used to correlate these parameters to both engine speeds and loads.

To normalize the variables and make the empirical relations more applicable to other engines, the following ratios are introduced:

$$v = \frac{Engine\ Speed}{Engine\ Speed\ at\ Maximum\ Torque}, \quad \mu = \frac{Applied\ External\ Torque}{Maximum\ Engine\ Torque}. \tag{2}$$

These ratios are substituted into the relations and the final shape of the equations describing the COVs of the IMEP, P_{max}, θ_{Pmax}, n_1 and n_2 are provided, as shown in Table 2.

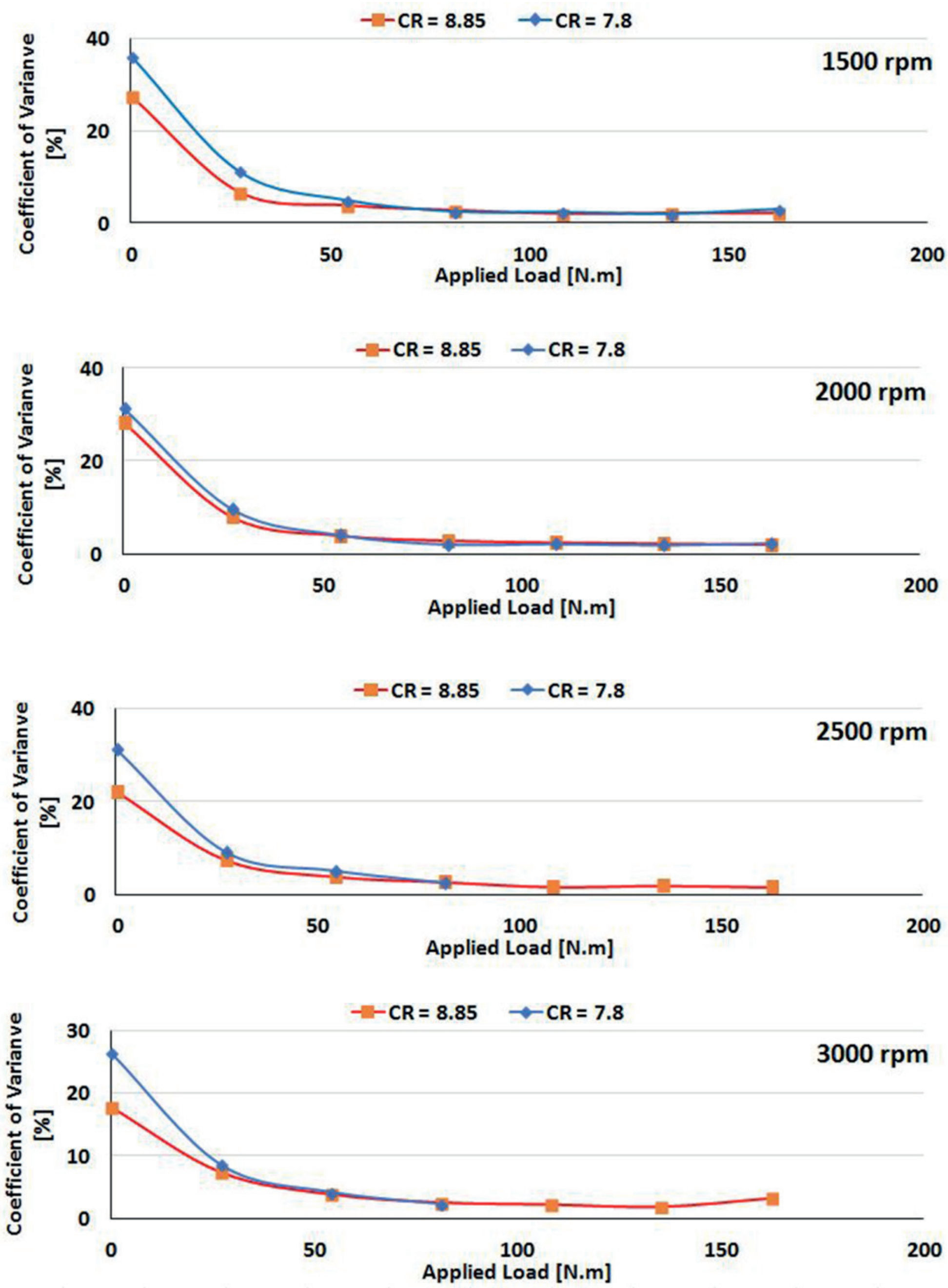

Figure 10 *Coefficient of the IMEP variance at two values of Compression Ratios (CR)*

These equations were used to calculate the COVs under the same measurements' conditions. The calculated results are confirmed by the measured values in Figure 9. For example, the COV_{IMEP} can be predicted within 98% accuracy, while P_{max} with 94% and so on as shown in Table 2 and Figure 9. The highest percentage of error is encountered at low load conditions.

3.3 Compression ratio effect on cyclic variability

Figure 10 presents a comparison of the measured COVs of IMEP at the compression ratio of 7.8 to those that were obtained with the initial compression ratio of 8.85. The figure proves that the dependence of the cyclic variability on the engine speed and load generally remains the same. However, with the lower compression ratio, the cyclic variability seems to increase at low loads, irrespective of the engine speed. This is attributed to the lower pressure and temperature at the end of the compression stroke, which eventually leads to longer delay periods and lower flame propagation speeds. The fresh charge, being slightly rich under the conditions of low load and the poor mixing at low speeds, can also increase the cyclic variability. Measurements could not be conducted for all the cases at high loads and speeds, at low compression ratios, as shown in Figure 10 at 2,500 and 3,000 rpm.

4 Conclusions

Extensive experimental work has been conducted to investigate the cyclic variability in spark-ignition engines. Conclusions can be summarized as follows:

1. Calculations of standard deviation of the COV_{IMEP} for different batches of successive cycles show that the optimum number of successive cycles, needed to be acquired to investigate the CCV problem, should be at least 300 cycles, at which the value of standard deviation starts to become constant. Previous works showed wide variations regarding that number starting from 42 up to 1,000 cycles.
2. Experimental results show that the COV are higher at lower loads and speeds (lower than $\mu = 16.5\%$ and $\nu = 41\%$, corresponding to 30 Nm load and 1,500 rpm speed in this engine respectively), due to low level of turbulence, poor mixing and higher residual gases. Moreover, the applied load has a dominant effect more than the engine speed in the cyclic variability problem, this is clear by checking the coefficients of relations illustrated in Figure (2).
3. By investigating the P-V curves for successive cycles it was found that the variations occur in six characterizing parameters, namely in-cylinder maximum pressure, the crank angle at which the maximum pressure occurs, compression and expansion polytropic indexes and suction and exhaust lines. The first four characterizing parameters exhibit the highest variations.
4. Novel empirical mathematical relations for IMEP and pressure characterizing parameters variation have been introduced (Table 2), as a function of applied load and speed, using an enormous amount of experimental data that were acquired at a high rate of 50 kHz.
5. The empirical relations were normalized to be applicable to any spark ignition engine by using the two dimensionless parameters ν and μ, instead of using absolute engine speed and applied load. Those relations give acceptable errors in predicted results compared to the measured ones.
6. In the case of a lower compression ratio, the cyclic variability seems to increase at low loads, irrespective of the engine speed.

These normalized empirical relations could be a useful tool in the early stages of engine design procedures and could be a guideline for cyclic variability control and assessment. However, other design and operating parameters, such as more compression ratio values, inlet conditions etc. need extensive investigation to introduce a complete map for cyclic variability.

Acknowledgement

The authors would like to thank the Department of Mechanical Power and Energy, Military Technical Collage for continuous support.

Conflicts of interest

The authors declare that they have no known competing financial interests or personal relationships that could have appeared to influence the work reported in this paper.

References

[1] HANUSCHKIN, A., SCHOBER, S., BODE, J., SCHORR, J., BOHM, B., KRUGER, CH., PETERS, S. Machine learning-based analysis of in-cylinder flow fields to predict combustion engine performance. *International Journal of Engine Research* [online]. 2019, **22**(1), p. 257-272. ISSN 1468-0874, eISSN 2041-3149. Available from: https://doi.org/10.1177/1468087419833269

[2] YOUNG, M. Cyclic dispersion in the engine - a literature survey. *SAE Technical Paper* [online]. 1981, 810020. ISSN 0148-7191, eISSN 2688-3627. Available from: https://doi.org/10.4271/810020

[3] MATEKUNAS, F. A. Modes and measures of cyclic combustion variability. *SAE Technical Paper* [online]. 1983, 830337. ISSN 0148-7191, eISSN 2688-3627. Available from: https://doi.org/10.4271/830337

[4] HEYWOOD, J. B. *Internal combustion engine fundamentals*. USA: McGraw-Hill, Inc., 1988. ISBN 0-07-028637-X.

[5] OZDOR, N., DULGER, M., SHER, E. Cyclic variability in spark ignition engines. A literature survey. *SAE Technical Paper* [online]. 1994, 940987. ISSN 0148-7191, eISSN 2688-3627. Available from: https://doi.org/10.4271/940987

[6] BAYRAKTAR, H. Theoretical investigation of flame propagation process in an SI engine running on gasoline-ethanol blends. *Renew. Energy* [online]. 2007, **32**(5), p. 758-771. ISSN 0960-1481, eISSN 1879-0682. Available from: https://doi.org/10.1016/j.renene.2006.03.017

[7] WANG, S., JI, C. Cyclic variation in a hydrogen-enriched spark-ignition gasoline engine under various operating conditions. *International Journal of Hydrogen Energy* [online]. 2012, **37**(1), p. 1112-1119. ISSN 0360-3199, eISSN 1879-3487. Available from: https://doi.org/10.1016/j.ijhydene.2011.02.079

[8] HANUSCHKIN, A., ZUNDORF, S., SCHMIDT, M., WELCH, C., SCHORR, J., PETERS, S., DREIZLER, A., BOHM, B. Investigation of cycle-to-cycle variations in a spark-ignition engine based on a machine learning analysis of the early flame kernel. *Proceedings of the Combustion Institute* [online]. 2020, **38**(4), p. 5751-5759. ISSN 1540-7489, eISSN 1873-2704. Available from: https://doi.org/10.1016/j.proci.2020.05.030

[9] HILL, P. G. Cyclic variations and turbulence structure in spark-ignition engines. *Combustion and Flame* [online]. 1988, **72**(1), p. 73-89. ISSN 0010-2180, eISSN 1556-2921. Available from: https://doi.org/10.1016/0010-2180(88)90098-3

[10] KAZMOUZ, S. J., HAWORTH, D. C., LILLO, P., SICK, V. Large-eddy simulations of a stratified-charge direct-injection spark-ignition engine: comparison with experiment and analysis of cycle-to-cycle variations. *Proceedings of the Combustion Institute* [online]. 2021, **38**(4), p. 5665-5672. ISSN 1540-7489, eISSN 1873-2704. Available from: https://doi.org/10.1016/j.proci.2020.08.035

[11] KAMMERMANN, T., MEROTTO, L., BLEINER, D., SOLTIC, P. Spark-induced breakdown spectroscopy for fuel-air equivalence ratio measurements at internal combustion engine-relevant conditions. *Spectrochimica Acta Part B: Atomic Spectroscopy* [online]. 2019, **155**, p. 79-89, ISSN 0584-8547, eISSN 1873-3565. Available from: https://doi.org/10.1016/j.sab.2019.03.006

[12] BOETTCHER, P. A., MEVEL, R., THOMAS, V., SHEPHERD, J. E. The effect of heating rates on low-temperature hexane air combustion. *Fuel* [online]. 2012, **96**, p. 392-403. ISSN 0016-2361, eISSN 1873-7153. Available from: https://doi.org/10.1016/j.fuel.2011.12.044

[13] ZUO, Z., ZHU, Z., LIANG, K., BAO, X., ZENG, D., KONG, L. Impact of dilution on laminar burning characteristics of premixed methane-dissociated methanol-air mixtures. *Fuel* [online]. 2021, **288**, 119741, ISSN 0016-2361, eISSN 1873-7153. Available from: https://doi.org/10.1016/j.fuel.2020.119741

[14] ZHANG, X., HUANG, Z., ZHANG, Z., ZHENG, J., YU, W., JIANG, D. Measurements of laminar burning velocities and flame stability analysis for dissociated methanol-air-diluent mixtures at elevated temperatures and pressures. *International Journal of Hydrogen Energy* [online]. 2009, **34**(11), p. 4862-4875. ISSN 0360-3199, eISSN 1879-3487. Available from: https://doi.org/10.1016/j.ijhydene.2009.03.046

[15] LIAO, S. Y., JIANG, D. M., HUANG, Z. H., CHENG, Q., GAO, J., HU, Y. Approximation of flammability region for natural gas-air-diluent mixture. *Journal of Hazardous Materials* [online]. 2005, **125**(1-3), p. 23-28. ISSN 0304-3894, eISSN 1873-3336. Available from: https://doi.org/10.1016/j.jhazmat.2005.05.021

[16] PUNDIR, B. P., ZVONOW, V. A., GUPTA, C. P. Effect of charge non-homogeneity on cycle-by-cycle variations in combustion in SI engines. *SAE Technical Paper* [online]. 1981, 810774. ISSN 0148-7191, eISSN 2688-3627. Available from: https://doi.org/10.4271/810774

[17] ZHU, Z., GU, H., ZHUB, Z., WEI, Y., ZENG, K., LIU, S. Investigation on mixture formation and combustion characteristics of a heavy-duty SI methanol engine. *Applied Thermal Engineering* [online]. 2021, **196**, 117258. ISSN 1359-4311, eISSN 1873-5606. Available from: https://doi.org/10.1016/j.applthermaleng.2021.117258

[18] WANG, Y., WEI, H., ZHOU, L., ZHANG, X., ZHONG, L. Effects of reactivity inhomogeneities on knock combustion in a downsized spark-ignition engine. *Fuel* [online]. 2020, **278**, 118317. ISSN 0016-2361, eISSN 1873-7153. Available from: https://doi.org/10.1016/j.fuel.2020.118317

[19] JI, C., WANG, S., ZHANG, B. Effect of spark timing on the performance of a hybrid hydrogen-gasoline engine at lean conditions. *International Journal of Hydrogen Energy* [online]. 2010, **35**(5), p. 2203-2212. ISSN 0360-3199, eISSN 1879-3487. Available from: https://doi.org/10.1016/j.ijhydene.2010.01.003

[20] KARVOUNTZIS-KONTAKIOTIS, A., DIMARATOS, A., NTZIACHRISTOS, L., SAMARAS, Z. Exploring the stochastic and deterministic aspects of cyclic emission variability on a high-speed spark-ignition engine. *Energy* [online]. 2017, **118**, p. 68-76. ISSN 0360-5442, eISSN 1873-6785. Available from: https://doi.org/10.1016/j.energy.2016.12.026

[21] OZDOR, N., DULGER, M., SHER, E. An experimental study of the cyclic variability in spark-ignition engines. *SAE Technical Paper* [online]. 1996, 412. ISSN 0148-7191, eISSN 2688-3627. Available from: https://doi.org/10.4271/960611

[22] ALEIFERIS, P. G., TAYLOR, A. M. K. P., WHITELAW, J. H., ISHII, K., URATA, Y. Cyclic variations of initial flame kernel growth in a Honda VTEC-E lean-burn spark-ignition engine. *SAE Technical Paper* [online]. 2000, 724. ISSN 0148-7191, eISSN 2688-3627. Available from: https://doi.org/10.4271/2000-01-1207

[23] SJERIC, M., KOZARAC, D., TATSCHL, R. Modelling of early flame kernel growth towards a better understanding of cyclic combustion variability in SI engines. *Energy Conversion and Management* [online]. 2015, **103**, p. 895-909. ISSN 0196-8904, eISSN 1879-2227. Available from: https://doi.org/10.1016/j.enconman.2015.07.031

[24] JUNG, D., SASAKI, K., SUGATA, K., MATSUDA, M., YOKOMORI, T., IIDA, N. Combined effects of spark discharge pattern and tumble level on cycle-to-cycle variations of combustion at lean limits of SI engine operation. *SAE Technical Paper* [online]. 2017, 2017-01-0677. ISSN 0148-7191, eISSN 2688-3627. Available from: https://doi.org/10.4271/2017-01-0677

[25] ABDEL-REHIM, A. A. Impact of spark plug number of ground electrodes on engine stability. *Ain Shams Engineering Journal* [online]. 2013, **4**(2), p. 307-316. ISSN 2090-4479, eISSN 2090-4495. Available from: https://doi.org/10.1016/j.asej.2012.09.006

[26] CRAVER, R. J., PODIAK, R. S., MILLER, R. D., CRAVER, R. J., PODIAK, R. S., MILLER, R. D. Spark plug design factors and their effect on engine performance spark plug design factors and their effect on engine performance. *SAE Technical Paper* [online]. 1970, 1970-02-01. ISSN 0148-7191, eISSN 2688-3627. Available from: https://doi.org/10.4271/700081

[27] HILL, P. G., KAPIL, A. The relationship between cyclic variations in spark-ignition engines and the small structure of turbulence. *Combustion and Flame* [online]. 1989, **78**(2), p. 237-247. ISSN 0010-2180, eISSN 1556-2921. Available from: https://doi.org/10.1016/0010-2180(89)90128-4

[28] RAVI, K., KHAN, M. A., BHASKER, J. P., PORPATHAM, E. Effects of spark plug configuration on combustion and emission characteristics of an LPG fuelled lean burn SI engine. *IOP Conference Series: Materials Science and Engineering* [online]. 2017, **263**(6), 062070. ISSN 1757-8981, eISSN 1757-899X. Available from: https://doi.org/10.1088/1757-899X/263/6/062070

[29] CHEN, L., WEI, H., ZHANG, R., PAN, J., ZHOU, L., FENG, D. Effects of spark plug type and ignition energy on combustion performance in an optical SI engine fueled with methane. *Applied Thermal Engineering* [online]. 2019, **148**, p. 188-195. ISSN 1359-4311, eISSN 1873-5606. Available from: https://doi.org/10.1016/j.applthermaleng.2018.11.052

[30] BERTSCH, M., SCHREER, K., DISCH, C., BECK, K. W., SPICHER, U. Investigation of the flow velocity in the spark plug gap of a two-stroke gasoline engine using laser-doppler-anemometry. *SAE Technical Paper* [online]. 2011, 2011-11-08. ISSN 0148-7191, eISSN 2688-3627. Available from: https://doi.org/10.4271/2011-32-0529

[31] SAYAMA, S., KINOSHITA, M., MANDOKORO, Y., FUYUTO, T. Spark ignition and early flame development of lean mixtures under high-velocity flow conditions: An experimental study. *International Journal of Engine Research* [online]. 2019, **20**(2), p. 236-246. ISSN 1468-0874, eISSN 2041-3149. Available from: https://doi.org/10.1177/1468087417748517

[32] GALLONI, E. Analyses about parameters that affect cyclic variation in a spark-ignition engine. *Applied Thermal Engineering* [online]. 2009, **29**(5-6), p. 1131-1137. ISSN 1359-4311, eISSN 1873-5606. Available from: https://doi.org/10.1016/j.applthermaleng.2008.06.001

[33] WANG, Y., ZHANG, J., WANG, X., DICE, P., SHAHBAKHTI, M., NABER, J., CZEKALA, M., QU, Q., GARLAN HUBERTS, G. Investigation of impacts of spark plug orientation on early flame development and combustion in a DI optical engine. *SAE International Journal of Engines* [online]. 2017, **10**(3), p. 995-1010. ISSN 1946-3936, e-ISSN 1946-3944. Available from: https://doi.org/10.4271/2017-01-0680

[34] ZHAO, L., MOIZ, A. A., SOM, S., FOGLA, N., BYBEEM, M., WAHIDUZZAMAN, S., MIRZAEIAN, M., MILLO, F., KODAVASAL, J. Examining the role of flame topologies and in-cylinder flow fields on cyclic variability in spark-ignited engines using large-eddy simulation. *International Journal of Engine Research* [online]. 2018, **19**(8), p. 886-904. ISSN 1468-0874, eISSN 2041-3149. Available from: https://doi.org/10.1177/1468087417732447

[35] TAMADONFAR, P., GULDER, O. L. Effects of mixture composition and turbulence intensity on flame front structure and burning velocities of premixed turbulent hydrocarbon/air Bunsen flames. *Combustion and Flame* [online]. 2015, **162**(12), p. 4417-4441. ISSN 0010-2180, eISSN 1556-2921. Available from: https://doi.org/10.1016/j.combustflame.2015.08.009

[36] NISHIYAMA, A., LE, M. K., FURUI, T., IKEDA, Y. The relationship between in-cylinder flow-field near spark plug areas, the spark behavior and the combustion performance inside an optical S.I. engine. *Applied Sciences* [online]. 2019, **9**(8), p. 1-13. eISSN 2076-3417. Available from: https://doi.org/10.3390/app9081545

[37] URUSHIHARA, T., MURAYAMA, T., TAKAGI, Y., LEE, K. H. Turbulence and cycle-by-cycle variation of mean velocity generated by swirl and tumble flow and their effects on combustion. *SAE Technical Paper* [online]. 1995, 412, ISSN 0148-7191, eISSN 2688-3627. Available from: https://doi.org/10.4271/950813

[38] LE COZ, J. F. Cycle-to-cycle correlations between flow field and combustion initiation in an S.I. engine. *SAE Technical Paper* [online]. 1992, 920517. ISSN 0148-7191, eISSN 2688-3627. Available from: https://doi.org/10.4271/920517

[39] MATSUDA, M., YOKOMORI, T., IIDA, N. Investigation of cycle-to-cycle variation of turbulent flow in a high-tumble SI engine. *SAE Technical Paper* [online]. 2017, 2017-01-2210. ISSN 0148-7191, eISSN 2688-3627. Available from: https://doi.org/10.4271/2017-01-2210

[40] REUSS, D. L. Cyclic variability of large-scale turbulent structures in directed and undirected IC engine flows. *SAE Technical Paper* [online]. 2000, 724. ISSN 0148-7191, eISSN 2688-3627. Available from: https://doi.org/10.4271/2000-01-0246

[41] BADE SHRESTHA, S. O., KARIM, G. A. Considering the effects of cyclic variations when modeling the performance of a spark-ignition engine. *SAE Technical Paper* [online]. 2001, 724. ISSN 0148-7191, eISSN 2688-3627. Available from: https://doi.org/10.4271/2001-01-3600

[42] MANZIE, C., WATSON, H. C., BAKER, P. Modeling the effects of combustion variability for application to idle speed control in SI engines. *SAE Technical Paper* [online]. 2002, 724. ISSN 0148-7191, eISSN 2688-3627. Available from: https://doi.org/10.4271/2002-01-2734